Circadian regulation of SARS-CoV-2 infection in lung epithelial cells

Xiaodong Zhuang[1*], Senko Tsukuda[1*], Florian Wrensch[2*], Peter AC Wing[1,3], Helene Borrmann[1], James M Harris[1], Sophie B Morgan[4], Laurent Mailly[2], Nazia Thakur[5], Carina Conceicao[5], Harshmeena Sanghani[6], Laura Heydmann[2], Charlotte Bach[2], Anna Ashton[7], Steven Walsh[7], Tiong Kit Tan[8], Lisa Schimanski[3,8], Kuan-Ying A Huang[9], Catherine Schuster[2], Koichi Watashi[10,11], Timothy SC Hinks[4], Aarti Jagannath[6], Sridhar R Vausdevan[7], Dalan Bailey[5], Thomas F Baumert[2,12] and Jane A McKeating[1,3].

Shared first authorship*

Corresponding author: Jane A McKeating, Tel: +44(0)1865 612894.
Email: jane.mckeating@ndm.ox.ac.uk and ORCID ID: 0000-0002-7229-5886.

1. Nuffield Department of Medicine, University of Oxford, Oxford, UK.
2. Université de Strasbourg, Strasbourg, France and INSERM, U1110, Institut de Recherche sur les Maladies Virales et Hépatiques, Strasbourg, France.
3. Chinese Academy of Medical Sciences (CAMS) Oxford Institute (COI), University of Oxford, Oxford, UK.
4. Respiratory Medicine Unit and National Institute for Health Research Oxford Biomedical Research Centre, Nuffield Department of Medicine, Experimental Medicine, University of Oxford, UK.
5. The Pirbright Institute, Ash Road, Pirbright, Woking, Surrey, UK.
6. Nuffield Department of Clinical Neurosciences, University of Oxford, Oxford, UK.
7. Department of Pharmacology, University of Oxford, Oxford, UK.
8. MRC Human Immunology Unit, MRC Weatherall Institute, John Radcliffe Hospital, Oxford 17 OX3 9DS, UK.
9. Research Center for Emerging Viral Infections, College of Medicine, Chang Gung University and Division of Pediatric Infectious Diseases, Department of Pediatrics, Chang Gung Memorial Hospital, Taoyuan, Taiwan.
10. Department of Virology II, National Institute of Infectious Diseases, Tokyo 162-8640, Japan.
11. Department of Applied Biological Science, Tokyo University of Science, Noda 278-8510, Japan.
12. Pole Hépato-digestif, IHU, Hopitaux Universitaires de Strasbourg, Strasbourg, France.

Key words: SARS-CoV-2, ACE2, Circadian, COVID-19
Characters with spaces: 19,969 of allowed 25,000

ABSTRACT

The COVID-19 pandemic, caused by SARS-CoV-2 coronavirus, is a global health issue with unprecedented challenges for public health. SARS-CoV-2 primarily infects cells of the respiratory tract, via binding human angiotensin-converting enzyme (ACE2)[1,2,] and infection can result in pneumonia and acute respiratory distress syndrome. Circadian rhythms coordinate an organisms response to its environment and recent studies report a role for the circadian clock to regulate host susceptibility to virus infection[3]. Influenza A infection of arhythmic mice, lacking the circadian component BMAL1, results in higher viral replication[4] and elevated inflammatory responses leading to more severe bronchitis[5,6], highlighting the impact of circadian pathways in respiratory function. We demonstrate circadian regulation of ACE2 in lung epithelial cells and show that silencing BMAL1 or treatment with the synthetic REV-ERB agonist SR9009 reduces ACE2 expression and inhibits SARS-CoV-2 entry and RNA replication. Treating infected cells with SR9009 limits viral replication and secretion of infectious particles, showing that post-entry steps in the viral life cycle are influenced by the circadian system. Our study suggests new approaches to understand and improve therapeutic targeting of COVID-19.

Circadian signalling exists in nearly every cell and is primarily controlled by a series of transcription/translation feedback loops. The transcriptional activators BMAL1 and CLOCK regulate thousands of transcripts including their own repressors, REV-ERBα and REV-ERBβ, that provide a negative feedback loop to control gene expression **(Fig.1a)**. To investigate a role for circadian pathways in the SARS-CoV-2 life cycle we initially assessed whether infection was time-dependent in synchronised Calu-3 lung epithelial cells (**Supplementary Fig.1**). Infecting Calu-3 cells at different circadian times (CT) with SARS-CoV-2 (**Fig.1b**) showed a rhythmic pattern of viral replication (**Fig.1c**). To assess whether this was mediated at the level of virus entry we used lentiviral pseudoparticles (pp) expressing the SARS-CoV-2 Spike glycoprotein and showed time-dependent infection (**Fig.1d**). We showed that SARS-CoV-2pp infection of Calu-3 cells was dependent on Spike-ACE2 interaction by blocking virus uptake with a receptor mimic (ACE2-Fc) or by neutralizing infection with anti-Spike mAb FI-3A (**Supplementary Fig.2**). Pseudoparticles bearing the vesicular stomatitis virus (VSV) glycoprotein infected the cells with comparable efficiency at all time points (**Fig.1d**). These data uncover a role for circadian-signalling pathways to regulate Calu-3 epithelial cell susceptibility to SARS-CoV-2 uptake.

Since ACE2 and transmembrane protease serine 2 (TMPRSS2) co-regulate SARS-CoV-2 internalization[1,2] we measured their expression in synchronised Calu-3 cells. ACE2 protein levels varied over 24h, with the trough (CT6) and peak (CT18) of expression associating with SARS-CoV-2pp entry (**Fig.2a**). In contrast, TMPRSS2 expression was similar at all time points sampled (**Fig.2a**). The classical model of circadian regulation is one of transcriptional control, however PCR quantification of ACE2 and TMPRSS2 transcripts showed no evidence of a rhythmic pattern in Calu-3 cells (**Fig.2b**), consistent with post-transcriptional regulation of ACE2. To extend these observations we quantified *Ace2* and *Tmprss2* transcripts in lung, liver and intestine harvested from light/dark entrained mice and observed limited evidence for a circadian pattern of expression (**Supplementary Fig.3**). Immunoblotting of ACE2 in the murine lung resulted in multiple bands of varying molecular weight, compromising the interpretation of these experiments. To further explore the role of circadian pathways in regulating ACE2 we shRNA silenced Bmal1, the major circadian transcriptional activator, and showed reduced ACE2 expression but a negligible effect on TMPRSS2 in Calu-3 cells (**Fig.2c**). To assess the impact of Bmal1 on SARS-CoV-2pp entry we infected the silenced Calu-3 cells and showed a significant reduction in pp infection, whereas

VSV-Gpp infection was unaffected (**Fig.2d**). During the COVID-19 pandemic several Spike variants have emerged; some conferring a fitness advantage to viral entry. D614G, has become prevalent in many countries, consistent with a reported fitness advantage for infecting cells of the upper respiratory tract[7,8]. SARS-CoV-2 Spike has a unique furin cleavage site that mediates membrane fusion and deletion of this motif has been observed both *in vitro*[9] and in animal models of infection[10]. Importantly, pp containing either Spike variant showed reduced infection of Bmal1 silenced Calu-3 cells (**Fig.2d**). In summary, these data show a circadian regulation of ACE2 that significantly impacts SARS-CoV-2 entry.

The availability of a synthetic agonist (SR9009) that activates REV-ERB and modulates circadian pathways[11,12] prompted us to investigate its role in SARS-CoV-2 infection. Treating Calu-3 cells with SR9009 reduced BMAL1 promoter activity and protein expression, with no impact on cell viability (**Supplementary Fig.4**). SR9009 treatment reduced ACE2 in a dose-dependent manner but had no effect on TMPRSS2 expression (**Fig.3a**). Importantly, SR9009 inhibited SARS-CoV-2pp infection in a BMAL1-dependent manner (**Fig.3b**). As expected from our earlier results, VSV-Gpp infection was insensitive to SR9009 treatment (**Fig.3b**). SR9009 was equally effective at limiting entry of pp bearing the D614G or Furin-KO Spike variants (**Fig.3c**). Using an independent pseudoparticle system based on VSV[1], we showed that SR9009 treatment of Calu-3 (**Fig.3d**) or VERO cells (**Supplementary Fig.5**) reduced particle infection. To extend our observations to a more physiologically relevant system, we showed that treating primary bronchial epithelial cells with SR9009 significantly reduced SARS-CoV-2pp infection (**Fig.3e**). SARS-CoV-2 Spike binding to ACE2 can induce formation of multicellular syncytia[13-15] and we established a real-time assay to measure cell-cell fusion[16]. Treating target cells with SR009 reduced both ACE2 expression (**Fig.3f**) and Spike driven cell-cell fusion (**Fig.3g**). In summary, these demonstrate that REV-ERB agonists repress ACE2 expression and limit SARS-CoV-2 entry and cell-cell fusion.

BMAL1 and REV-ERB regulate gene expression by binding E-box or ROR response elements (RORE), respectively, in the promoter and enhancer regions of their target genes[17,18]. A genome-wide CRISPR screen identified 153 host factors that are important in SARS-CoV-2 infection[19] and bio-informatic analysis[20] identified 144 canonical E-box motifs 'CANNTG' and 80 ROR response elements 'RGGTCA' in these genes (**Fig.4a**). Furthermore, analysing murine transcript data from BMAL1 ChIP-seq[21] and REV-ERB knock-out animals[22] identified putative target genes and suggested that ~30% of SARS-CoV-2 host factors are BMAL1 or REV-ERB targets (**Fig.4a**), suggesting a role for circadian pathways in SARS-CoV-2 RNA replication. To test this hypothesis we validated our earlier pseudoparticle data with an authentic viral replication system and demonstrate a significant reduction of SARS-CoV-2 (Victoria 01/20 strain) replication in *Bmal1* silenced Calu-3 compared to parental cells (**Fig.4b**). Furthermore, SR9009 treatment significantly reduced SARS-CoV-2 replication, assessed by intracellular RNA and the secretion of infectious particles (**Fig.4c**). These observations were recapitulated with VERO cells (**Supplementary Fig.6**). To define whether circadian pathways regulate post-entry steps in the SARS-CoV-2 life cycle, we evaluated the effect of SR9009 on viral replication when added before or after virus inoculation. The agonist reduced viral RNA levels under both conditions (**Fig.4c**), leading us to conclude that both SARS-CoV-2 entry and replication are circadian regulated.

Our studies show circadian regulation of ACE2 in lung epithelial cells and show striking inhibitory effects of BMAL1 silencing and the synthetic REV-ERB agonist SR9009 treatment on ACE2 expression, SARS-CoV-2 entry and virus replication in lung epithelial cells. Of note, SARS-CoV-1 and alpha NL63 also require

ACE2 to enter cells[23] and our data support a role for circadian factors in regulating the infection of these related coronaviruses. The human *Ace2* promoter encodes putative binding sites for BMAL1/CLOCK and REV-ERB, however, we did not observe binding of these factors by chromatin immunoprecipitation-qPCR in Calu-3 cells (**Supplementary Fig.7**). In addition, there was no evidence for rhythmic expression of *Ace2* transcripts in Calu-3 or in the lung, liver or intestine from entrained mice, consistent with bio-informatic analyses of published diurnal/circadian datasets from baboons[24] and mice[25]. These results are consistent with recent studies showing a role for post-transcriptional and post-translational mechanisms in regulating the circadian clock[26-28]. There is an emerging role of microRNAs (miRNAs) in modulating the circadian clock[29,30] and miRNAs have been reported to regulate ACE2 expression[31], providing a possible post-transcriptional mechanism. Our studies show ACE2 to be a rhythmically 'moving' target and this could be relevant for evaluating new treatments targeting this step in the viral life cycle.

In addition to the circadian regulation of ACE2-mediated viral entry, we observed a marked suppression of SARS-CoV-2 RNA and genesis of infectious particles following SR9009 treatment and in Bmal1 silenced cells. Our bio-informatic analysis suggests that 30% of SARS-CoV-2 host factors are potentially BMAL1/REV-ERB regulated, highlighting a role for circadian-signalling to influence multiple steps in the SARS-CoV-2 life cycle. Further work is needed to characterise the circadian-dependent mechanisms of SARS-CoV-2 repression. A key finding from our study is the potential application of chronomodifying drugs for the treatment of COVID-19[32]. Dexamethasone is one of the few drugs that can reduce the severity of COVID-19[33] and is known to synchronise circadian pathways[34-36]. Over the last decade, a number of compounds that target core clock proteins have been developed[37], including REV-ERB[38,39] and RORs[40,41] agonists that have been shown to inhibit hepatitis C virus and HIV replication[42,43]. A report demonstrating REV-ERB dependent and independent effects of SR9009[44] suggests some additional off-target effects. We cannot exclude the possibility of additional pathways contributing to SR9009 anti-viral activity; however, our use of genetic targeting approaches confirms a role for BMAL1 in regulating SARS-CoV-2 replication. REV-ERBα agonists can also impact the host immune response by suppressing IL-6[45] and so may offer a 'two pronged' approach to reduce viral replication and adverse host immune responses.

Circadian clocks can also impact on the pharmacokinetics and pharmacodynamics of drug responses[46]. Epidemiological[47-49] and molecular evidence[50] shows that night shift workers suffer circadian disruption and are at an increased risk of developing chronic inflammatory diseases. Identifying whether shift work is a risk factor for acquiring SARS-CoV-2 infection or developing moe severe disease could inform public health policy. Our observations raise questions as to how our *in vitro* studies translate to humans, where the time of exposure to SARS-CoV-2 may impact on the likelihood of infection, the host response, virus shedding, transmission and disease severity and are worthy of further investigation.

FIGURE LEGENDS

Figure 1. SARS-CoV-2 is circadian regulated.

(**a**) Circadian transcription–translation feedback loops control daily rhythmic expression of circadian genes. The molecular clock generates a cycle of 24-hour periodicity where a heterodimeric transcription factor BMAL1-CLOCK activates the transcription from E-box sequences in target gene promoters. Gene products feedback to repress the transcriptional activity of the heterodimeric activator. Ligand activation of REV-ERB represses the transcription of Bmal1. (**b**) Circadian infection protocol. (**c**) Calu-3 cells were synchronized by serum shock, inoculated with SARS-CoV-2 at an MOI of 0.1 or 0.01 for 1h and viral RNA measured after 24h. RNA levels are expressed relative to CT0; mean ± S.E.M., n = 2. (**d**) Calu-3 cells were serum shocked and synchronised cells inoculated with SARS-CoV-2pp or VSV-Gpp for 2h with luciferase activity measured 24h later. Data expressed relative to CT0; mean ± S.E.M., n = 6-12, Kruskal–Wallis test with Dunn's multiple comparisons.

Figure 2. Circadian regulation of ACE2 dependent SARS-CoV-2 infection.

(a) Synchronised Calu-3 cells were assessed for ACE2, TMPRSS2 and BMAL1 expression together with housekeeping β-actin by western blotting; data are representative of two experiments. Densitometric analysis quantified ACE2 and TMPRSS2 in individual samples and normalized to their own β-actin loading control. SARS-CoV-2pp infection values from Fig.1d were plotted as a dotted line to illustrate concordance with ACE2 expression levels. (**b**) Synchronized Calu-3 cells were assessed for *ACE2*, *TMPRSS2* and *BMAL1* mRNA by qRT-PCR and expressed relative to CT0; data are the average of two independent experiments. (**c**) Calu-3 cells were transduced with lentivirus encoding shBmal1 or control and ACE2, TMPRSS2, BMAL1 and β-actin protein expression assessed by western blotting after 24 h. (**d**) Control or shBmal1 treated cells were infected with lentiviral pseudotypes expressing wild type (WT) or mutant (D614G or Furin KO) Spike variants or with VSV-Gpp. Viral entry (luciferase activity) was measured 24h later and data expressed relative to WT (mean ± S.E.M., n = 4-6, Mann–Whitney test).

Figure 3. REV-ERB agonist reduces ACE2 dependent SARS-CoV-2 entry and cell-cell fusion.

(**a**) Calu-3 cells were treated with SR9009 (5 or 10 μM) for 24h and assessed for ACE2 and TMPRSS2 expression together with housekeeping β-actin by western blotting. **(b)** Control or shBmal1 silenced Calu-3 cells were treated with SR9009 for 24h followed by infection with SARS-Cov-2pp or VSV-Gpp. After 24h viral entry was assessed by measuring luciferase activity and expressed relative to untreated cells (mean ± S.E.M., n = 3, Kruskal–Wallis ANOVA with Dunn's test). **(c)** Control or SR9009 treated Calu-3 cells were infected with SARS-CoV-2 wild type (WT), D614G or furin mutant pp. Viral entry was expressed relative to untreated cells 24h later (mean ± S.E.M., n = 4-6, Kruskal–Wallis ANOVA with Dunn's test). **(d)** Control or SR9009 treated Calu-3 cells were infected with SARS2-S-VSVpp and 24h later luciferase activity measured and data expressed relative to untreated cells (mean ± S.E.M., n = 3). Stats not needed for dose curves **(e)** Primary Bronchial Epithelial Cells (PBECs) were treated with SR9009 (20 μM) for 24h prior to SARS-CoV-2pp infection. Viral entry was measured as luciferase activity and data presented as mean ± S.E.M of triplicate wells from three independent donors relative to untreated control cells, Paired two-tailed t test. **(f)** SR9009 treated Huh-7 cells were assessed for ACE2 expression together with the housekeeping gene β-actin. **(g)** Huh-7 target cells expressing a split rLuc-GFP reporter (8-11) were treated overnight with SR9009 at the indicated concentrations or with DMSO vehicle (Ctrl.) before culturing with Spike expressing HEK-293T cells with the split rLuc-GFP (1-7) and SR9009 added

for the indicated times. A representative image of SARS-CoV-2 Spike induced syncytia at 3 days post co-culture is shown (left panel). GFP-positive syncytia were quantified every 4h using an IncuCyte real-time imaging platform (right panel). Five fields of view were obtained per well at 10x magnification and GFP expression quantified by calculating the total GFP area using the IncuCyte analysis software.

Figure 4. REV-ERB agonist inhibits SARS-CoV-2 replication post-entry.

(**a**) Overlap between SARS-CoV-2 host factors and BMAL1 or REV-ERB regulated genes. Sequence analysis of promoters of genes encoding SARS-CoV-2 host genes with HOMER (Hypergeometric Optimization of Motif EnRichment tool) identifies a canonical E-box motif 'CANNTG' in 144 of the 153 genes and an ROR response element 'RCGTCA' in 80. (**b**) Bmal1 silencing reduces SARS-CoV-2 RNA. Calu-3 cells were transduced with lentivirus encoding shBmal1 or a control followed by SARS-Cov2 infection. Viral RNA was measured and expressed relative to control cells (mean ± S.E.M., n = 4-6, Mann–Whitney test). (**c**) Calu-3 cells were treated with 20 μM SR9009 either 24h before infection or from 2h post-inoculation with SARS-CoV-2. Cells were incubated for 22h, intracellular viral RNA quantified by qPCR and expressed relative to the untreated control. Infectivity of the extracellular viral particles was assessed by plaque assay using VERO cells. Data are presented as mean ± S.E.M. from n=3 independent biological replicates. Statistical significance was determined using Kruskal–Wallis ANOVA with Dunn's test.

STAR METHODS

Materials. All reagents and chemicals were obtained from Sigma-Aldrich (now Merck) unless stated otherwise. REV-ERB agonist SR9009 was purchased from Calbiochem, US, dissolved in dimethyl sulfoxide (DMSO) and cytotoxicity determined by a Lactate dehydrogenase (LDH) assay (Promega, UK) or MTT assay (Sigma, UK). The BMAL1 promoter was amplified from genomic DNA using forward primer: 5'-CCGCTCGAGGGGACAACGG CGAGCTCGCAG-3' with reverse primer: 5'-CCCAAGCTTCGGCGGCGGCGGCGGCAAGTC-3' and cloned into the pGL3 luciferase reporter vector (Promega, UK). The lenti-shBmal1 plasmid was purchased from Abmgood (UK). Recombinant ACE2-Fc was previously reported[51].

Cell culture. Calu-3, Huh-7, HEK293T and VERO E6 cells were cultured in DMEM supplemented with 10% fetal bovine serum (FBS), 2mM L-glutamine, 100 U/mL penicillin and 10µg/mL streptomycin (all reagents from Life Technologies/Thermo Fisher). VERO E6/TMPRSS2 cells (a VERO E6 cell line stably overexpressing the TMPRSS2 gene, kindly provided by Dr Makoto Takeda at Department of Virology III, National Institute of Infectious Diseases[52]) were cultured in DMEM supplemented with 10% fetal bovine serum, 10 units/mL penicillin, 10 mg/mL streptomycin, 10 mM HEPES (pH 7.4), and 1 mg/mL G418 (Life Technologies, UK). All cell lines were maintained at 37°C and 5% CO_2 in a standard culture incubator. Human PBECs were obtained using flexible fibreoptic bronchoscopy from healthy control volunteers under light sedation with fentanyl and midazolam. Participants provided written informed consent. The study was reviewed by the Oxford Research Ethics Committee B (18/SC/0361). Airway epithelial cells were taken using 2mm diameter cytology brushes from 3rd to 5th order bronchi and cultured in Airway Epithelial Cell medium (PromoCell, Heidelberg, Germany) in submerged culture.

SARS-CoV-2 pseudoparticle genesis and infection. SARS-CoV-2 lentiviral pp were generated by transfecting HEK-293T cells with p8.91 (Gag-pol), pCSFW (luciferase reporter) and a codon optimised expression construct pcDNA3.1-SARS-CoV-2-Spike, as previously reported[53]. The Furin cleavage site mutant was generated by mutagenesis of a pcDNA3.1 based clone expressing a C-terminally flag-tagged SARS-CoV-2 Spike protein (Wuhan-Hu-1 isolate; MN908947.3). The polybasic cleavage site TNSPRRA in SARS-CoV-2 Spike was replaced with the corresponding SARS-CoV variant sequence SLL. The pNBF SARS-CoV2 FL D614G mutant was a kind gift from Dr. Daniel Watterson and Dr. Naphak Modhiran at the University of Queensland. Supernatants containing viral pp were harvested at 48 and 72h post-transfection, frozen and stored at -80°C. As a control pp were generated that lacked a viral envelope glycoprotein (No Env) and were included in all infection experiments to control for non-specific uptake. This control was included in all pp experiments and the luciferase values obtained subtracted from values acquired with the SARS-CoV-2pp. To confirm spike-dependent infection, SARS-CoV-2pp were incubated with the anti-S-mAb FI-3A (1µg/mL)[54] for 30 min prior to infection for all experiments.

SARS-CoV-2 VSV pp were generated as previously reported[1] using reagents provided by Stefan Pöhlmann (Infection biology unit, German Primate Center, Göttingen, Germany). Briefly, HEK-293T cells were transfected with an expression construct encoding a c-terminal truncated version of SARS-CoV-2-S for assembly into VSV pp (pCG1-SARS-CoV-2-S-ΔC)[55]. After 24h, the transfected cells were infected with a replication-incompetent VSV (VSV*ΔG[56]) containing GFP and firefly luciferase reporter genes, provided by Gert Zimmer (Institute of Virology and Immunology, Mittelhäusern, Switzerland). After 1h, the cells

were washed with PBS before medium containing a VSV-G antibody (I1, mouse hybridoma supernatant from CRL-2700, ATCC) and supernatants harvested after 24h. The VSV*ΔG used for generating the pps was propagated in BHK-21 G43 cells stably expressing VSV-G. Viral titres were determined by infecting Calu-3 cells and measuring cellular luciferase after 48h.

SARS-CoV-2 propagation and infection. For infection experiments, the SARS-CoV-2 (Victoria 01/20 isolate) obtained from Public Health England was propagated in Vero E6 cells. Naïve Vero E6 cells were infected with SARS-CoV-2 at an MOI of 0.003 and incubated for 48-72h until visible cytopathic effects were observed. Culture supernatants were harvested, clarified by centrifugation to remove residual cell debris and stored at -80°C before measuring the infectious titre by plaque assay. Briefly, Vero E6 cells were inoculated with serial dilutions of SARS-CoV-2 stocks for 2h followed by addition of a semi-solid overlay consisting of 3% carboxymethyl cellulose (SIGMA). Cells were incubated for 72h, plaques enumerated by fixing cells using amido black stain and plaque-forming units (PFU) per mL calculated. For infection of Calu-3 cells, cells were plated 24h before infecting with the stated MOI. Cells were inoculated with virus for 2h after which the unbound virus was removed by washing three times with with phosphate buffered saline (PBS). Unless otherwise stated, infected cells were maintained for 24h before harvesting for downstream applications.

SARS-CoV-2 cell-cell fusion assay. The SARS-CoV-2 cell-cell fusion assay was performed as described previously[16]. Briefly, HEK-293T Lenti rLuc-GFP 1-7 (effector cells) and Huh-7.5 Lenti rLuc-GFP 8-11 (target cells) cells were seeded separately at $7.5x10^5$ per well in a 6 well dish in 3mL of phenol-red free DMEM, supplemented with 10% FBS, 1% sodium pyruvate and 1% penicillin/streptomycin (10,000 U/mL) before culturing overnight at 37°C, 5% CO_2. The effector cells were transfected with a plasmid expressing SARS-CoV-2 Spike or a blank vector. Meanwhile, target cells were diluted to $2x10^5$/mL and 100µL seeded into a clear, flat-bottomed 96 well plate and mock-treated or treated with SR9009 (3µM or 7µM). The following day, the effector cells were harvested, diluted to $2x10^5$/mL and 100µL cultured with the drug/target cell mix, with SR9009 concentrations maintained at 3µM or 7µM. To quantify GFP expression, cells were imaged every 4h using an IncuCyte S3 live cell imaging system (Essen BioScience). Five fields of view were obtained per well at 10x magnification and GFP expression determined by calculating the total GFP area using the IncuCyte analysis software.

Oligonucleotides:

qPCR Primers (5'-3')
Human ACE2 forward: GGGATCAGAGATCGGAAGAAGAAA
Human ACE2 reverse: AGGAGGTCTGAACATCATCAGTG
Human TMPRSS2 forward: AGGTGAAAGCGGGTGTGAGG
Human TMPRSS2 reverse: ATAGCTGGTGGTGACCCTGAG
Human B2M forward: CTACACTGAATTCACCCCCACTG
Human B2M reverse: ACCTCCATGATGCTGCTTACATG
Human BMAL1: TaqMan Gene Expression Assay, ThermoFisher, Hs00154147
Mouse Ace2 forward: AATTCCACTGAAGCTGGGCA
Mouse Ace2 reverse: CCATTCAGTGTTCCACCCCA
Mouse Tmprss2 forward: CTCAGGCAACGTTGACC
Mouse Tmprss2 reverse: GTCTCCTGGTGAGGCATTCA

Mouse Bmal1 forward: AAGTGCAACAGGCCTTCAGT
Mouse Bmal1 reverse: GGTGGCCAGCTTTTCAAATA
Mouse GAPDH: TaqMan Gene Expression Assay, ThermoFisher, Hs99999905_m1
SARS-CoV-2_N forward: CACATTGGCACCCGCAATC
SARS-CoV-2_N reverse: GAGGAACGAGAAGAGGCTTG
ChIP-PCR Primers (5'-3')
Per1 promoter forward: GTCAAGGAAAATCCCCAGCTTCTG
Per1 promoter reverse: CCAAGATTGGTGACGTAAATGCCA
Bmal1 promoter forward: TTGGGCACAGCGATTGGT
Bmal1 promoter reverse: GTAAACAGGCACCTCCGTCC
ACE2 promoter Ebox1 forward: AGCATCACAAGAAACCTATAGGCA
ACE2 promoter Ebox1 reverse: TGCCTCCACTATTGCTTTTAGAC
ACE2 promoter Ebox2 forward: TGTCCACTGCTTTTCCTTATTCCA
ACE2 promoter Ebox2 reverse: TGCCTATAGGTTTCTTGTGATGCT
ACE2 promoter Ebox3 forward: TGGCAGGGTTCAAGGGCCTACC
ACE2 promoter Ebox3 reverse: TGGAATAAGGAAAAGCAGTGGACA
ACE2 promoter Ebox4/5 forward: GGCTACAGAGGATCAGGAGTTGACA
ACE2 promoter Ebox4/5 reverse: TGCCTCCTTCTCCTTCACTTACCT
ACE2 promoter Ebox6 forward: AACTTAGCTGGGCGTGGTGGTG
ACE2 promoter Ebox6 reverse: CGCGATCTCGGCTCACTGCAAG
ACE2 promoter RORE1 forward: GGCTACAGAGGATCAGGAGTTGACA
ACE2 promoter RORE1 reverse: TGCCTCCTTCTCCTTCACTTACCT
ACE2 promoter RORE2 forward: TGCAAAGGCAGATCAGGAGAGT
ACE2 promoter RORE2 reverse: GCCACTGTGCCCAGCCATTTCT
ACE2 promoter RORE3 forward: GCACTTTGGGAGGCCGAGTTGG
ACE2 promoter RORE3 reverse: CACCACCACGCCCAGCTAAGTT

RT-qPCR. Cells were washed in PBS then lysed using Tri-reagent (Sigma), and mRNA extracted by phase separation. Equal amounts of cDNA were synthesised using the High Capacity cDNA Kit (Applied Biosystems) and mRNA expression determined using Fast SYBR master mix in a StepOne thermocycler (Applied Biosystems) using the $\Delta\Delta C_t$ method. The lung tissues were lysed in TRI Reagent (Sigma) using a gentleMACS dissociator and RNA extracted using the manufacturers protocol. cDNAs were synthesized using the Maxima H Minus cDNA Synthesis Kit (Thermo Scientific) and mRNA quantified using iTaq Universal SYBR Green Supermix (Biorad) and specific primers on a QuantStudio 3 RT-PCR system (Applied Biosystems).

Immunoblotting. Cell lysates were prepared by washing cells with PBS, then lysed in Igepal lysis buffer (10mM Tris pH 7.5, 0.25M NaCl, 0.5% Igepal) supplemented with protease inhibitor cocktail (Roche Complete™) at 4°C for 5 min, followed by clarification by centrifugation (3 min, 12,000 rpm). Supernatant was mixed with Laemmli sample buffer, separated by SDS-PAGE and proteins transferred to polyvinylidene difluoride membrane (Immobilon-P, Millipore). Membranes were blocked in 5% milk in PBS/0.1% Tween-20, then incubated with anti-ACE2 (Abcam ab108252), anti-TMPRSS2 (SCBT sc-515727), anti-BMAL1 (Abcam Ab93806) or Anti-β-actin (Sigma A5441) primary antibodies and

appropriate HRP-conjugated secondary antibodies (DAKO). Chemiluminescence substrate (West Dura, 34076, Thermo Fisher Scientific) was used to visualize proteins using a ChemiDoc XRS+ imaging system (BioRad). Anti-β-actin-HRP conjugate (Abcam ab49900) and/or Coomassie brilliant blue staining was used to verify equal protein loading and densitometric analysis performed using ImageJ software (NIH).

Bioinformatics. The published 153 SARS-CoV-2 host factors were converted to Entrez gene names[19]. BMAL1 regulated genes were obtained from the published BMAL1 ChIP-seq in the mouse liver[21]. REV-ERB regulated genes were defined from published liver-specific loss of the REV-ERB paralogues[22]. Promoters (-1kb from TSS) of genes encoding SARS-CoV-2 host factors were analyzed with the HOMER (Hypergeometric Optimization of Motif EnRichment) tool for motif discovery (E-box motif CANNTG; RORE motif RGGTCA).

Chromatin immuno-Precipitation (ChIP) and quantitative PCR: $1x10^7$ Calu-3 cells were harvested from 80% confluent 15cm plates and fixed with 1% formaldehyde (Sigma Aldrich 47608) for 10 min at room temperature before quenching with 125 mM glycine. Cells were washed twice with ice cold PBS, pelleted (800rpm, 10 min 4°C) and lysed in 500µl of Nuclear Extraction buffer (10 mM Tris pH 8.0, 10 mM NaCl, 1% NP-40) supplemented with a protease inhibitor cocktail (Roche Complete™). Samples were diluted 1:1 in ChIP Dilution Buffer (0.01% SDS, 1.1% Triton, 0.2mM EDTA; 16.7 mM Tris pH8.1, 167mM NaCl) and pulse sonicated using a Bioruptor R sonicator (Diagenode, U.K.) at high power for 15 min at 4°C (15 sec on, 15 sec off). Sonicated lysates were clarified by centrifugation at 1300 rpm for 10 min and precleared with Protein A agarose beads (Millipore, 16-156). Samples were immunoprecipitated with primary anti-BMAL1 (ChIP grade, Abcam Ab3350) or anti-REV-ERBα (ChIP grade, Abcam Ab181604) or IgG control mAb and precipitated with Protein A agarose beads. Precipitates were washed in low salt buffer (0.1% SDS, 1% Triton, 2 mM EDTA, 20 mM Tris pH8.1, 150mM NaCl), high salt buffer (0.1% SDS, 1% Triton, 2mM EDTA, 20 mM Tris pH 8.1, 500 mM NaCl), LiCl Buffer (1% Igepal, 1mM EDTA, 10 mM Tris pH 8.1, 250 mM LiCl, 1% sodium deoxycholate) and finally twice in TE wash buffer (10 mM Tris pH8.0, 1mM EDTA) before being eluted from the beads in 240µL of elution buffer (0.1 M $NaHCO_3$, 1% SDS). Complexes were reverse crosslinked in a heated shaker at 65°C overnight, 1400 rpm, in the presence of 200 mM NaCl. Eluates were treated with Proteinase K (SIGMA) and RNaseA (SIGMA) before cleanup using MiniElute PCR Purification columns (Qiagen). Samples were analysed on a LightCycler96 (Roche) using SYBR green qPCR mastermix (PCR Biosystems, UK). Fold enrichment was calculated for each sample relative to their own IgG controls.

Animals. Mouse experiments were carried out at the Institute of Viral and Liver Disease animal facility (approval number E-67-482-7). C57BL/6J male mice were purchased from Charles River and housed in individually ventilated cages under a 12/12 dark/light cycle with a ZT0 corresponding to 7am. After two weeks of acclimatisation, nine-week-old mice were sacrificed at different time points (ZT0, ZT4, ZT8, ZT12, ZT16, ZT20; n = 5/time point). Organs were harvested after exsanguination by intracardiac puncture, frozen in liquid nitrogen and kept at -80°C until further processing.

Statistical Analysis. All data are presented as mean values ± SEM. P values were determined using Mann-Whitney testing (two group comparisons) or with a Kruskal–Wallis ANOVA (multi group comparisons) using PRISM version 9. In the figures $*$ denotes $p < 0.05$, $**$ < 0.01, *** <0.001, **** <0.0001, n.s. denotes non-significant.

DATA AVAILABILITY

The authors declare that all data supporting the findings of this study are available within the article and its Supplementary Information files or are available from the authors upon request.

AUTHOR CONTRIBUTIONS

XZ designed and conducted experiments and co-wrote MS; ST designed and conducted experiments and co-wrote MS; FW designed and conducted experiments; PACW designed and conducted experiments; HB conducted experiments and analysed data; JMH ran bio-informatic analysis; SBM provided PBECs; LM provided resources; LH and CB conducted experiments; CS designed and analyzed experiments; NZ conducted experiments; CC conducted experiments; HS designed and conducted experiments; LH conducted experiments; CB conducted experiments; AA conducted experiments; SW conducted analysis; TKH provided reagents; LS provided reagents; K-YAH provided reagents; KW provided experimental data; TSCH provided reagents; AJ provided experimental data; SV experimental data; DB designed and conducted experiments and provided reagents; TFB designed and analyzed experiments, provided reagents and co-wrote MS; JAM designed the study and co-wrote the MS.

ACKNOWLEDGEMENTS AND FUNDING

The authors would like to thank colleagues for the provision of reagents: Anderson Ryan (Oncology Department, University of Oxford) for Calu-3 cells; Pramila Rijal and Alain Townsend for anti-S neutralizing mAb F1-3A and ACE2-Fc (WIMM, Oxford). Daniel Watterson, Keith Chappell, Ariel Isaacs and Naphak Modhiran (University of Queensland) for the Spike D614G mutant. Additional thanks to Darren Blase and Zuzana Bencokova for facilitating virus work in NDMRB. We would like to thank Romain Martin and Nicolas Brignon for excellent technical assistance and Atish Mukherji for helpful discussions. The McKeating laboratory is funded by a Wellcome Investigator Award (IA) 200838/Z/16/Z, UK Medical Research Council (MRC) project grant MR/R022011/1 and Chinese Academy of Medical Sciences (CAMS) Innovation Fund for Medical Science (CIFMS), China (grant number: 2018-I2M-2-002). The Hinks laboratory is funded by grants from the Wellcome (104553/z/14/z, 211050/Z/18/z) and the National Institute for Health Research (NIHR) Oxford Biomedical Research Centre; the views expressed are those of the authors and not those of the NHS or NIHR. Aarti Jagannath is funded by David Phillips fellowship from BBSRC-UKRI (BB/N01992X/1). The Baumert lab is funded by grants from the FRM and ANR TargEnt-COVID-19, Inserm, the University of Strasbourg, the Institut Universitaire de France and the Agence Nationale de Recherche sur le Sida et les hépatites virales (ANRS), the National Institute of Allergy and Infectious Diseases of the National Institutes of Health under award number U19AI12386, ERC AdG HEPCIR, the European Union's Horizon 2020 research and innovation programme under grant agreement No 671231, FONDATION ARC TheraHCC2.0 and Fondation ARC pour la recherche sur le cancer (grant n° IHU201901299).

CONFLICTS OF INTEREST

The other authors declare no financial interests.

REFERENCES

1. Hoffmann, M.*, et al.* SARS-CoV-2 Cell Entry Depends on ACE2 and TMPRSS2 and Is Blocked by a Clinically Proven Protease Inhibitor. *Cell* **181**, 271-280 e278 (2020).
2. Wan, Y., Shang, J., Graham, R., Baric, R.S. & Li, F. Receptor Recognition by the Novel Coronavirus from Wuhan: an Analysis Based on Decade-Long Structural Studies of SARS Coronavirus. *J Virol* **94**(2020).
3. Borrmann, H., McKeating, J.A. & Zhuang, X. The Circadian Clock and Viral Infections. *Journal of biological rhythms*, 748730420967768 (2020).
4. Edgar, R.S.*, et al.* Cell autonomous regulation of herpes and influenza virus infection by the circadian clock. *Proc Natl Acad Sci U S A* **113**, 10085-10090 (2016).
5. Sengupta, S.*, et al.* Circadian control of lung inflammation in influenza infection. *Nature communications* **10**, 4107 (2019).
6. Ehlers, A.*, et al.* BMAL1 links the circadian clock to viral airway pathology and asthma phenotypes. *Mucosal Immunol* **11**, 97-111 (2018).
7. Korber, B.*, et al.* Tracking Changes in SARS-CoV-2 Spike: Evidence that D614G Increases Infectivity of the COVID-19 Virus. *Cell* **182**, 812-827 e819 (2020).
8. Drew Weissman, M.-G.A., Tushan de Silva, Paul Collini, Hailey Hornsby, Rebecca Brown, Celia C LaBranche, Robert J Edwards, Laura Sutherland, Sampa Santra, Katayoun Mansouri, Sophie Gobeil, Charlene McDanal, Norbert Pardi, Nick Hengartner, Paulo J.C. Lin, Ying Tam, Pamela A Shaw, Mark G Lewis, Carsten Boesler, Ugur Sahin, Priyamvada Acharya, Barton F Haynes, Bette Korber, David C Montefiori. D614G Spike Mutation Increases SARS CoV-2 Susceptibility to Neutralization. *medrxiv* (2020).
9. Davidson, A.D.*, et al.* Characterisation of the transcriptome and proteome of SARS-CoV-2 reveals a cell passage induced in-frame deletion of the furin-like cleavage site from the spike glycoprotein. *Genome Med* **12**, 68 (2020).
10. Thomas P. Peacock, D.H.G., Jie Zhou, Laury Baillon, Rebecca Frise, Olivia C. Swann , Ruthiran, Kugathasan, Rebecca Penn, Jonathan C. Brown, Raul Y. Sanchez-David, Luca Braga, Maia Kavanagh Williamson, Jack A. Hassard, Ecco Staller, Brian Hanley, Michael Osborn, Mauro Giacca, Andrew D. Davidson, David A. Matthews and Wendy S. Barclay. The furin cleavage site of SARS-CoV-2 spike protein is a key determinant for transmission due to enhanced replication in airway cells. *bioRxiv* (2020).
11. Trump, R.P.*, et al.* Optimized chemical probes for REV-ERBalpha. *Journal of medicinal chemistry* **56**, 4729-4737 (2013).
12. Solt, L.A.*, et al.* Regulation of circadian behaviour and metabolism by synthetic REV-ERB agonists. *Nature* **485**, 62-68 (2012).
13. Stadlmann, S., Hein-Kuhnt, R. & Singer, G. Viropathic multinuclear syncytial giant cells in bronchial fluid from a patient with COVID-19. *Journal of clinical pathology* **73**, 607-608 (2020).
14. Rockx, B.*, et al.* Comparative pathogenesis of COVID-19, MERS, and SARS in a nonhuman primate model. *Science* **368**, 1012-1015 (2020).
15. Xu, Z.*, et al.* Pathological findings of COVID-19 associated with acute respiratory distress syndrome. *The Lancet. Respiratory medicine* **8**, 420-422 (2020).
16. Thakur, N.*, et al.* Micro-fusion inhibition tests: quantifying antibody neutralization of virus-mediated cell-cell fusion. *The Journal of general virology* (2020).

17. Harding, H.P. & Lazar, M.A. The orphan receptor Rev-ErbA alpha activates transcription via a novel response element. *Molecular and cellular biology* **13**, 3113-3121 (1993).
18. Forman, B.M.*, et al.* Cross-talk among ROR alpha 1 and the Rev-erb family of orphan nuclear receptors. *Molecular endocrinology* **8**, 1253-1261 (1994).
19. Daniloski, Z.*, et al.* Identification of Required Host Factors for SARS-CoV-2 Infection in Human Cells. *Cell* (2020).
20. Heinz, S.*, et al.* Simple combinations of lineage-determining transcription factors prime cis-regulatory elements required for macrophage and B cell identities. *Molecular cell* **38**, 576-589 (2010).
21. Beytebiere, J.R.*, et al.* Tissue-specific BMAL1 cistromes reveal that rhythmic transcription is associated with rhythmic enhancer-enhancer interactions. *Genes & development* **33**, 294-309 (2019).
22. Cho, H.*, et al.* Regulation of circadian behaviour and metabolism by REV-ERB-alpha and REV-ERB-beta. *Nature* **485**, 123-127 (2012).
23. Li, F. Receptor recognition mechanisms of coronaviruses: a decade of structural studies. *J Virol* **89**, 1954-1964 (2015).
24. Mure, L.S.*, et al.* Diurnal transcriptome atlas of a primate across major neural and peripheral tissues. *Science* **359**(2018).
25. Zhang, Z.*, et al.* Genome-wide effect of pulmonary airway epithelial cell-specific Bmal1 deletion. *FASEB J* **33**, 6226-6238 (2019).
26. Reddy, A.B.*, et al.* Circadian orchestration of the hepatic proteome. *Curr Biol* **16**, 1107-1115 (2006).
27. Kojima, S., Shingle, D.L. & Green, C.B. Post-transcriptional control of circadian rhythms. *J Cell Sci* **124**, 311-320 (2011).
28. Mauvoisin, D. Circadian rhythms and proteomics: It's all about posttranslational modifications! *Wiley Interdiscip Rev Syst Biol Med* **11**, e1450 (2019).
29. Pegoraro, M. & Tauber, E. The role of microRNAs (miRNA) in circadian rhythmicity. *Journal of genetics* **87**, 505-511 (2008).
30. Park, I.*, et al.* microRNA-25 as a novel modulator of circadian Period2 gene oscillation. *Experimental & molecular medicine* **52**, 1614-1626 (2020).
31. Widiasta, A.*, et al.* Potential role of ACE2-related microRNAs in COVID-19-associated nephropathy. *Non-coding RNA research* **5**, 153-166 (2020).
32. Sengupta, S.*, et al.* Clocks, viruses and immunity: lessons for the COVID-19 pandemic. *Journal of biological rhythms* ***In press***(2021).
33. Group, R.C.*, et al.* Dexamethasone in Hospitalized Patients with Covid-19 - Preliminary Report. *N Engl J Med* (2020).
34. Oster, H.*, et al.* The circadian rhythm of glucocorticoids is regulated by a gating mechanism residing in the adrenal cortical clock. *Cell Metab* **4**, 163-173 (2006).
35. Oster, H.*, et al.* The Functional and Clinical Significance of the 24-Hour Rhythm of Circulating Glucocorticoids. *Endocr Rev* **38**, 3-45 (2017).
36. Pezuk, P., Mohawk, J.A., Wang, L.A. & Menaker, M. Glucocorticoids as entraining signals for peripheral circadian oscillators. *Endocrinology* **153**, 4775-4783 (2012).
37. Ercolani, L.*, et al.* Circadian clock: Time for novel anticancer strategies? *Pharmacol Res* **100**, 288-295 (2015).

38. Wang, S., Li, F., Lin, Y. & Wu, B. Targeting REV-ERBalpha for therapeutic purposes: promises and challenges. *Theranostics* **10**, 4168-4182 (2020).
39. Everett, L.J. & Lazar, M.A. Nuclear receptor Rev-erbalpha: up, down, and all around. *Trends in endocrinology and metabolism: TEM* **25**, 586-592 (2014).
40. Solt, L.A. & Burris, T.P. Action of RORs and their ligands in (patho)physiology. *Trends in endocrinology and metabolism: TEM* **23**, 619-627 (2012).
41. Hirota, T.*, et al.* Identification of small molecule activators of cryptochrome. *Science* **337**, 1094-1097 (2012).
42. Zhuang, X.*, et al.* The circadian clock components BMAL1 and REV-ERBalpha regulate flavivirus replication. *Nature communications* **10**, 377 (2019).
43. Borrmann, H.*, et al.* Pharmacological activation of the circadian component REV-ERB inhibits HIV-1 replication. *Scientific reports* **10**, 13271 (2020).
44. Dierickx, P.*, et al.* SR9009 has REV-ERB-independent effects on cell proliferation and metabolism. *Proc Natl Acad Sci U S A* **116**, 12147-12152 (2019).
45. Gibbs, J.E.*, et al.* The nuclear receptor REV-ERBalpha mediates circadian regulation of innate immunity through selective regulation of inflammatory cytokines. *Proc Natl Acad Sci U S A* **109**, 582-587 (2012).
46. Ruben, M.D., Smith, D.F., FitzGerald, G.A. & Hogenesch, J.B. Dosing time matters. *Science* **365**, 547-549 (2019).
47. Wegrzyn, L.R.*, et al.* Rotating Night-Shift Work and the Risk of Breast Cancer in the Nurses' Health Studies. *Am J Epidemiol* **186**, 532-540 (2017).
48. Vyas, M.V.*, et al.* Shift work and vascular events: systematic review and meta-analysis. *BMJ* **345**, e4800 (2012).
49. Pan, A., Schernhammer, E.S., Sun, Q. & Hu, F.B. Rotating night shift work and risk of type 2 diabetes: two prospective cohort studies in women. *PLoS Med* **8**, e1001141 (2011).
50. Kervezee, L., Cuesta, M., Cermakian, N. & Boivin, D.B. Simulated night shift work induces circadian misalignment of the human peripheral blood mononuclear cell transcriptome. *Proc Natl Acad Sci U S A* **115**, 5540-5545 (2018).
51. Zhou, D.*, et al.* Structural basis for the neutralization of SARS-CoV-2 by an antibody from a convalescent patient. *Nature structural & molecular biology* **27**, 950-958 (2020).
52. Matsuyama, S.*, et al.* Enhanced isolation of SARS-CoV-2 by TMPRSS2-expressing cells. *Proc Natl Acad Sci U S A* **117**, 7001-7003 (2020).
53. Thompson, C.P.*, et al.* Detection of neutralising antibodies to SARS coronavirus 2 to determine population exposure in Scottish blood donors between March and May 2020. *MedRxiv* (2020).
54. Hauang, K.-Y.A.*, et al.* Plasmablast-derived antibody response to acute SARS-CoV-2 infection in humans. *BioRxiv* (2020).
55. Hoffmann, M., Kleine-Weber, H. & Pohlmann, S. A Multibasic Cleavage Site in the Spike Protein of SARS-CoV-2 Is Essential for Infection of Human Lung Cells. *Molecular cell* **78**, 779-784 e775 (2020).
56. Berger Rentsch, M. & Zimmer, G. A vesicular stomatitis virus replicon-based bioassay for the rapid and sensitive determination of multi-species type I interferon. *PloS one* **6**, e25858 (2011).

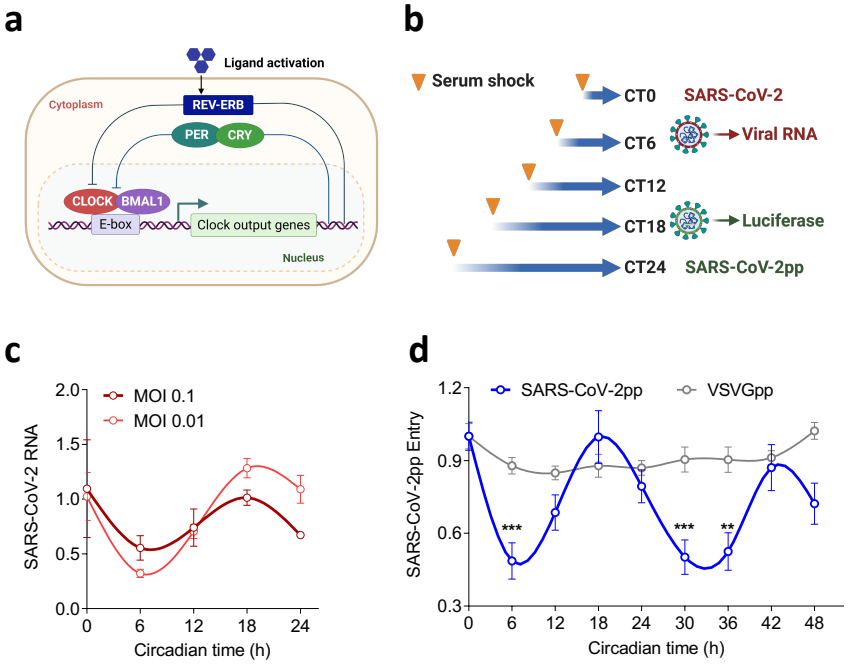

Figure 1. SARS-CoV-2 infection is circadian.

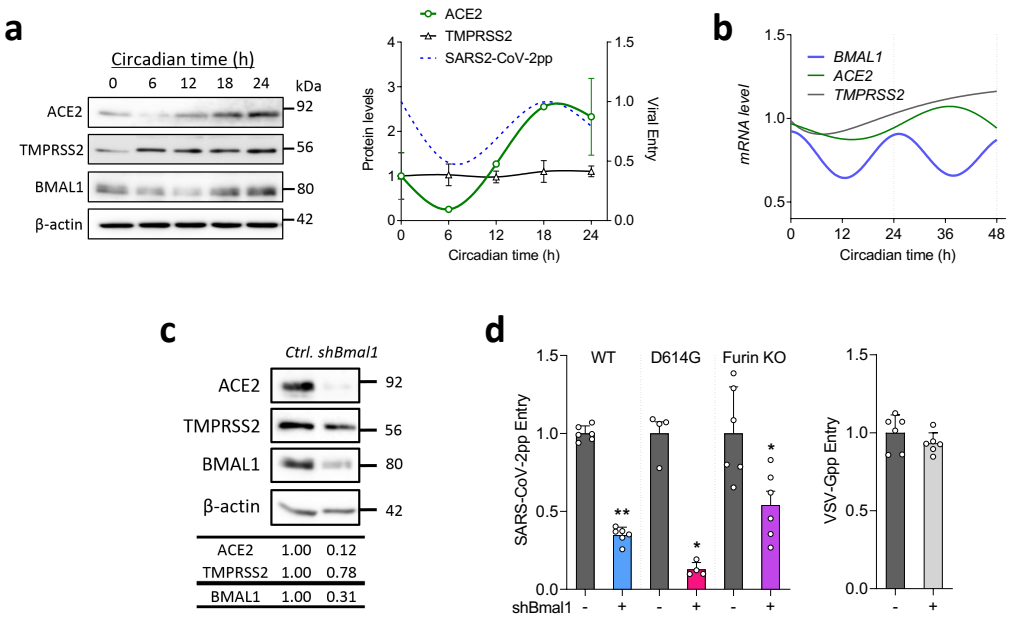

Figure 2. Circadian regulation of ACE2 dependent SARS-CoV-2 entry.

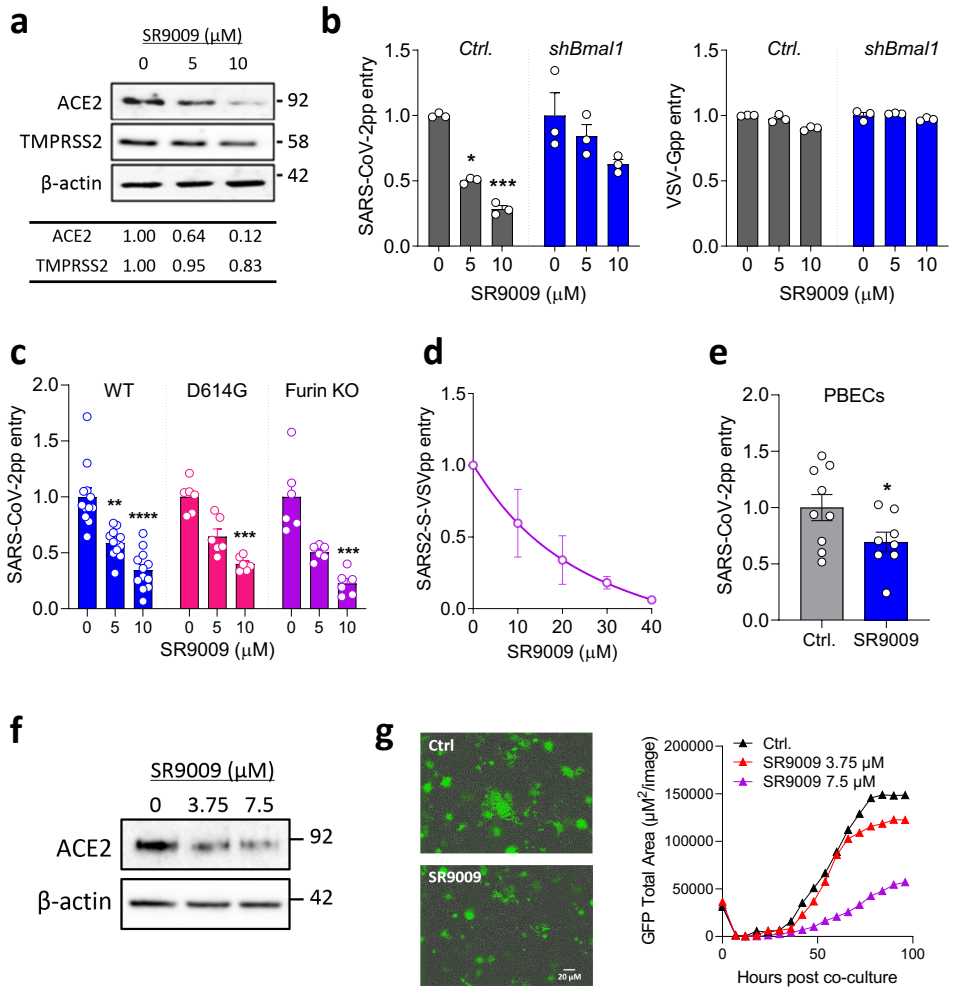

Figure 3. REV-ERB agonist reduces ACE2 dependent SARS-CoV-2 entry and cell-cell fusion.

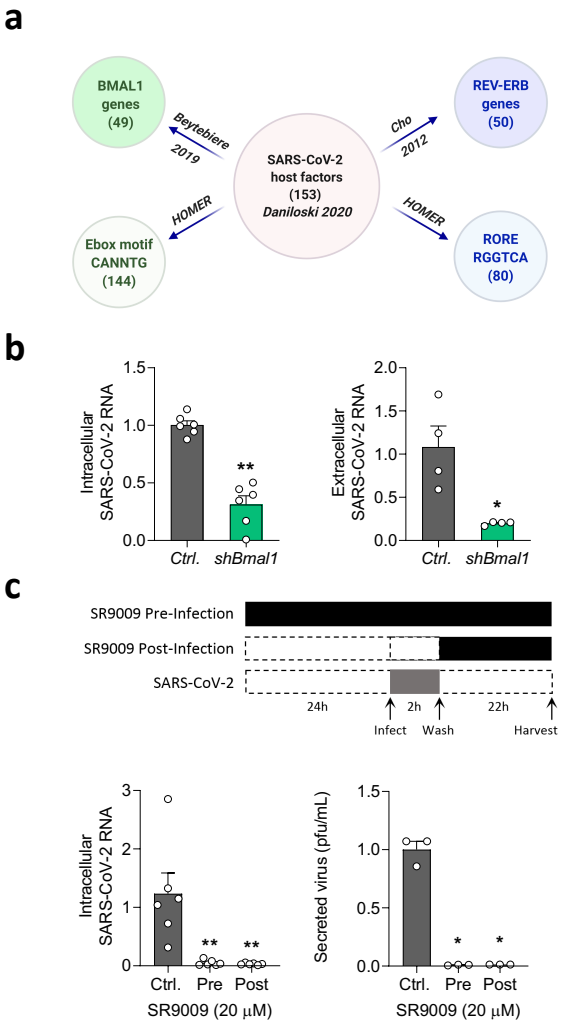

Figure 4. REV-ERB agonist inhibits SARS-CoV-2 replication post-entry.